A new Electromagnetic Model in SOLEDGE3X

Raffael Düll[1], Hugo Bufferand[1], Eric Serre[2], Guido Ciraolo[1], Gloria Falchetto[1], Virginia Quadri[1], Nicolas Rivals[1], Patrick Tamain[1], Hao Yang[1]

[1] *CEA-IRFM, Cadarache, St-Paul-Lèz-Durance, France*

[2] *M2P2, Aix-Marseille University, CNRS, Centrale Marseille, France*

Electromagnetic effects and micro-instabilities are known to play a key role in driving plasma turbulence in the pedestal region. In particular, they affect the filamentary structure of turbulent plasma blobs in the Scrape-off layer [1]. For more realistic simulations, it is thus desirable to integrate these effects into the physical model.

In its current form the 3D turbulent transport code SOLEDGE3X uses an electrostatic assumption with a fixed magnetic field. Perpendicular fluctuations of the magnetic field B can be derived from the local value of the magnetic vector potential in parallel direction $A_\parallel$, known from Ampère's law. To avoid unphysical speeds in the plasma, it is crucial to consider electron inertia [2] which requires solving for the time evolution of the parallel current density $j_\parallel$ in the generalized Ohm's law.

Therefore, we extend the physical model of SOLEDGE3X by the two fields $A_\parallel$ and $j_\parallel$. The original current balance equation (1) on the electric potential Φ is completed with Ohm's (2) and Ampère's (3) laws.

$$\nabla\cdot\left[\frac{m_\alpha n_\alpha}{B^2}\partial_t\nabla_\perp\Phi\right] = \nabla\cdot(j_\parallel\vec{b}) - \partial_t\Omega_\pi \tag{1}$$

$$j_\parallel + \frac{\sigma_\parallel m_e}{n_e e^2}\left(\frac{\partial j_\parallel}{\partial t} - \vec{\nabla}\cdot\left(\nu_e\vec{\nabla}_\perp j_\parallel\right)\right) = \sigma_\parallel\left(-\nabla_\parallel\Phi - \partial_t A_\parallel + \frac{T_e}{e}\nabla_\parallel\log(n_e) + \frac{1.71}{e}\nabla_\parallel T_e\right) \tag{2}$$

$$\Delta_\perp A_\parallel = -\mu_0 j_\parallel \tag{3}$$

$\partial_t\Omega_\pi$ contains further terms from the current balance and ν_e drives a diffusion on $j_\parallel$ for numerical stability. To contain the spread of numerical operators, $A_\parallel$ and $j_\parallel$ are calculated on toroidally and poloidally staggered cells. They are not defined on cells overlapping the domain boundary where $A_\parallel$ is forced to 0 and the sheath current $\left(1+\frac{\sigma_\parallel m_e}{n_e e^2}\partial_t\right) j_\parallel^{BC} = j_{sat}\left(1-e^{\Lambda-\Phi/T_e}\right)$ is applied by penalization on Φ in equation (1).

We solve the three fields implicitly in a coupled system. Using the reference plasma parameters $\beta_0 = \frac{e n_0 T_0}{B_0^2/\mu_0}$ and $\mu = \frac{\hat{\sigma}_\parallel m_e}{\hat{n}_e m_i}$ we obtain a full-domain 3D problem on the dedimensionalized discrete variables $\hat{\Phi}$ and $\hat{A}_\parallel$ at the new timestep $n+1$:

$$\begin{pmatrix} \frac{1}{\hat{\delta}t}\hat{\nabla}\cdot\left[\hat{D}_\perp\hat{\nabla}_\perp\circ\right]+\hat{\nabla}\cdot\left[\hat{D}_\parallel\hat{\nabla}_\parallel\circ\vec{b}\right] & \frac{\beta_0}{\hat{\delta}t}\hat{\nabla}\cdot\left[\hat{D}_\parallel\circ\vec{b}\right] \\ \hat{D}_\parallel\hat{\nabla}_\parallel\circ & \frac{\beta_0}{\hat{\delta}t}\hat{D}_\parallel\circ-\hat{\nabla}\cdot\left[\hat{\nabla}_\perp\circ\right] \end{pmatrix}\begin{pmatrix}\hat{\Phi}^{n+1}\\ \hat{A}_\parallel^{n+1}\end{pmatrix}=\begin{pmatrix}\hat{\nabla}\cdot\left[\hat{D}_t\hat{j}_\parallel^n\vec{b}\right]+RHS^\Phi\\ \hat{D}_t\hat{j}_\parallel^n+RHS^{A_\parallel}\end{pmatrix} \tag{4}$$

The coefficients herein are given by $\hat{D}_\perp=\frac{m_i n_i}{B^2}$, $\hat{D}_\parallel=\frac{\hat{\sigma}_\parallel}{1+\mu/\hat{\delta}t}$ and $\hat{D}_t=\frac{\mu}{\hat{\delta}t+\mu}$. Once solved, the new value for the parallel current $\hat{j}_\parallel^{n+1}$ is retrieved by means of Ohm's law (2). We employ an implicit Euler scheme with fixed timestep size $\hat{\delta}t$ in Eq. (4), nonetheless the code also encompasses higher-order time integration schemes with adaptive stepsize.

Because of the large conductivity $\hat{\sigma}_\parallel$ the double Laplacian operator on $\hat{\Phi}$ is inherently anisotropic. Adding the electron inertia term $\mu/\hat{\delta}t$ to the parallel diffusion coefficient $\hat{D}_\parallel$ always improves the matrix condition with an even greater effect at low timestep sizes. Numerical experiments using the LGMRES iterative scheme with the GAMG multigrid preconditionner by PETSc [3] confirm the condition improvement. Table 1 states the convergence speed and connected solve times for four stripped-down variants of the system (1) - (3).

	Φ	$\Phi - j_\parallel$	$\Phi - A_\parallel$	$\Phi - A_\parallel - j_\parallel$
Number of iterations	165	35	660	117
Solve time per iteration [s]	0.45	0.11	6.36	1.15
Total simulation time [s]	2268	1599	14275	3841

Table 1: *KSP convergence behaviour for different combinations of equations (1) – (3) on a 3D limiter case with ca. 500.000 cells over 1500 timesteps on 96 computing cores. There is no action of the potentials on the fluid quantities via drifts.*

The comparison between the original system with only Φ and the two-potential system $\Phi - A_\parallel$ shows that introducing the magnetic vector potential degrades the numerical and overall performance of the code. On the other side, the benefits of electron inertia effects on the anisotropy induce a significant improvement of the convergence properties.

To demonstrate the correct implementation of the staggered operators in equations (1) - (3), the method of manufactured solutions [4] allows to confront an analytic solution to the code output. The relevant plasma fields were initialized with an arbitrary profile on a curved 3D cylindrical geometry, and corresponding analytical source terms were calculated to maintain a steady-state solution throughout the simulation. The relative difference between the initial and any following plasma state then indicates the error incurred by the numerical scheme.

If now the number of grid points increases, the error should decrease at double the rate to recover the theoretical second-order discretization of the spatial operators. This behaviour is verified in Figure 1, where the calculated error almost perfectly matches the expected convergence depicted as dashed lines. For each scenario, the number of points per dimension was increased by a factor 1.3 and hence the total number by ca. 2.2.

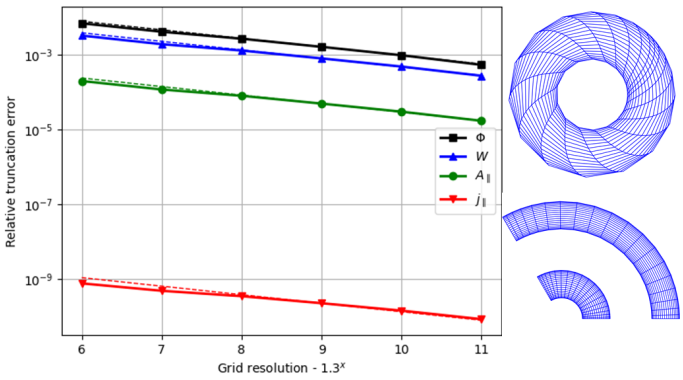

Figure 1: *Convergence of the MMS model. The shape of the used domain and mesh is shown to the right in the $\psi-\theta$ (top) and $\psi-\varphi$ (bottom) planes.*

The extended physical model should exhibit basic electromagnetic behaviour. If we now further let the electron density evolve over time, we obtain the system discussed in [5]:

$$\partial_t n_e = \frac{1}{e}\nabla\cdot j_{\parallel} \tag{5}$$

In equations (1) - (3) we ignore the vorticity terms $\partial_t\Omega_\pi$ and the diffusion on $j_{\parallel}$. The linear analysis of the system lets us expect a decaying standing wave on all four fields (n_e, Φ, $A_{\parallel}$, $j_{\parallel}$) with a phase shift. The common expected wave frequency is:

$$\omega_0^2 = \frac{v_A^2 + Kk_\perp^2}{1+Ck_\perp^2}k_{\parallel}^2 - \frac{\gamma^2 k_\perp^4}{4\left(1+Ck_\perp^2\right)^2} \tag{6}$$

For improved readability we introduced the helper variables $K=\frac{T_e}{en_e\mu_0}$ and $C=\frac{m_e}{e^2 n_i\mu_0}$ as well as the Alfvén group velocity $v_A=\frac{B}{\sqrt{m_i n_i\mu_0}}$ and a damping coefficient $\gamma=\frac{1}{\sigma_{\parallel}\mu_0}$. The squared parallel and perpendicular wavenumbers arise from the Fourier transforms of the respective diffusion operators:

$$\nabla\cdot\left(\vec{b}\cdot\nabla X\vec{b}\right)\sim k_{\parallel}^2 = \left(b_\theta k_\theta + b_\varphi k_\varphi\right)^2 \qquad \nabla\cdot\left(\nabla X - \vec{b}\cdot\nabla X\vec{b}\right)\sim k_\perp^2 = \left(k_\psi + k_\theta + k_\varphi\right)^2 - k_{\parallel}^2$$

From the parameter and domain choices, the second term in the dispersion relation (6) is negligible. A wave in the parallel direction then appears whose velocity approaches the Alfvén for small $k_\perp$ and the thermal electron velocity K/C for large $k_\perp$. The necessity of electron inertia effects pointed out in [2] becomes apparent as parallel wave speeds may reach nonphysical large values without the electronic constraint.

To validate the physical behaviour of the new model, we set up simulations to recover the transition from Alfvén to thermal electron waves in a similar fashion as in [6]. We consider a 3D slab

with periodic boundary conditions in all directions. There are hence no curvature effects, and we do not consider the diffusion on $j_\parallel$. The equilibrium magnetic field is uniform at 1T and has both a poloidal and a toroidal component. The electron density is initialized to its reference value 10^{19} m^{-3} with a small wave-shaped perturbation and one mode per direction. The remaining evolving fields Φ, $A_\parallel$, $j_\parallel$ are set to 0 at the simulation start and respond to the perturbation in n_e. The "parallel" domain dimensions L_θ and L_φ are fixed, and such is the parallel wavenumber $k_\parallel$. We then modify the "radial" domain length L_ψ to study several samples of $k_\perp$. If we fit the simulation results for each of the four fields to a complex wave function and compare the real parts to the predicted wave frequency ω_0 (the continuous line in Fig 2), we observe an excellent agreement.

Figure 2: *Transition between Alfvén and thermal electron waves.*

The vorticity equation on the electric potential Φ was extended with the parallel electromagnetic potential $A_\parallel$. The further addition of electron inertia effects on the parallel current $j_\parallel$ improves the convergence of the implicit solver and prevents the unrestrained growth of wave speeds for large perpendicular modes. The implementation was validated through an analytic solution, and basic electromagnetic behaviour could be observed on a slab case. The new model can now be used to investigate small perturbations of the magnetic equilibrium and their effect on turbulent transport.

References

[1] W. Lee, J. Angus, M. V. Umansky, and S. I. Krasheninnikov, Journal of Nuclear Materials **463**, (2015)

[2] B. D. Dudson, S. L. Newton, J. T. Omotani and J. Birch., Plasma Physics and Controlled Fusion **63**, 12(2021)

[3] S. Balay, W. Gropp, L. C. McInnes, and B. F Smith. ANL-2/17, (1998)

[4] P. J. Roache, Journal of Fluids Engineering **124**, (2021)

[5] B. Scott Plasma Phys. Control. Fusion **39**, (1997)

[6] A. Stegmeir, A. Ross, T. Body, M. Francisquez, W. Zholobenko, D. Coster, O. Maj, P. Manz, F. Jenko, B. N. Rogers and K. S. Kang. Physics of Plasmas **26**, 5(2019)